

In-beam spectroscopy of $^{215}\text{Rn}_{86}$

M. E. Debray,^{1,2} M. Davidson,³ J. Davidson,³ A. J. Kreiner,^{1,2,3} M. A. Cardona,^{1,2,3} D. Hojman,^{1,3} D. R. Napoli,⁴ S. Lenzi,⁵ G. de Angelis,⁴ M. De Poli,⁴ A. Gadea,⁴ D. Bazzacco,⁵ C. Rossi-Alvarez,⁵ N. Medina,⁶ and C. A. Ur⁵

¹*Departamento de Física, Comisión Nacional de Energía Atómica, Buenos Aires, Argentina*

²*Escuela de Ciencia y Tecnología, Universidad de San Martín, San Martín, Argentina*

³*CONICET, 1033 Buenos Aires, Argentina*

⁴*INFN, Laboratori Nazionali di Legnaro, Legnaro, Italy*

⁵*Dipartimento di Fisica, Sezione di Padova, Padova, Italy*

⁶*Departamento de Física Nuclear, Universidade de São Paulo, Brazil*

(Received 29 July 2011; revised manuscript received 4 May 2012; published 20 July 2012)

The yrast level structure of ^{215}Rn has been studied by means of in-beam spectroscopy α - γ - γ coincidence techniques through the $^{207}\text{Pb}(^{18}\text{O},2\alpha2n)$ reaction at 93 MeV bombarding energy, using the 8π GASP-ISIS spectrometer at Legnaro. New spectroscopic information has been obtained. The deduced low-lying level scheme of ^{215}Rn does not exhibit the alternating parity structure observed in the heavier known isotones ^{216}Fr , ^{217}Ra , ^{218}Ac , and ^{219}Th . From this result, the lightest nucleus showing evidence for octupole collectivity is ^{216}Fr , defining the lowest-mass corner for this kind of phenomenon as $N \geq 129$ and $Z \geq 87$.

DOI: [10.1103/PhysRevC.86.014326](https://doi.org/10.1103/PhysRevC.86.014326)

PACS number(s): 21.10.Re, 23.20.Lv, 25.70.Gh, 27.80.+w

I. INTRODUCTION

The region of the nuclear chart between the double closed-shell nucleus ^{208}Pb and the well deformed actinides is rich in structural changes. This region has become the object of numerous studies related to the discovery of very low-lying negative-parity collective states indicating the presence of an octupole instability. With four protons and three neutrons more than the doubly closed-shell nucleus ^{208}Pb ($N = 126$, $Z = 82$), ^{215}Rn is just at the edge of the region where octupole collectivity starts to occur. All the known heavier isotones with $N = 129$, namely ^{216}Fr [1], ^{217}Ra [2], ^{218}Ac [3,4], and ^{219}Th [5] present clear signals of quadrupole and octupole instability. In fact the transition between a spherical shell model (or single particle) and a collective regime seems to take place at $N = 129$. So far, the lightest nucleus showing evidence for octupole collectivity is ^{216}Fr , defining a lower boundary for this kind of phenomenon as $Z > 86$ and $N > 128$. In order to determine more precisely the Z and N values for which this collective regime starts to set in, we studied in the present work the next lighter odd isotone ^{215}Rn . We give here a more complete in-beam level scheme of ^{215}Rn and discuss the relation between its structure and that of its neighbors, in particular its heavier isotone ^{217}Ra . The hitherto known level structure of ^{215}Rn consists of a few levels obtained from the ^{219}Ra α decay [6,7]. The ground state of ^{215}Rn has been assigned as $9/2^+$ because it favors the α decay ($E_\alpha = 8.674$ MeV) to the $9/2^+$ ^{211}Po [8] ground state with a hindrance factor (HF) of 1.5.

II. EXPERIMENTAL PROCEDURES

The nucleus ^{215}Rn has been studied here through the $^{207}\text{Pb}(^{18}\text{O},2\alpha2n)$ reaction at 93 MeV bombarding energy using the 8π GASP-ISIS spectrometer at Legnaro. A 2 mg/cm² thick (backed by a 25 $\mu\text{g}/\text{cm}^2$ C foil) ^{207}Pb target was bombarded with a 10 p nA ^{18}O beam. The spectroscopy of nuclei in this

mass region is made difficult by the very small incomplete fusion cross sections [9] (in the used reaction of only few tens of a μb) and the intense background originating from fission. To reduce this intense γ fission background, we used the ISIS array (40 telescopic E - ΔE particle detectors) to trigger the GASP spectrometer [40 Compton-suppressed Ge detectors and a multiplicity filter of 80 bismuth germanate (BGO) elements], selecting the evaporation α particles emitted in coincidence with transitions between excited states in ^{215}Rn . This powerful technique has been used here to identify unambiguously the γ transitions belonging to ^{215}Rn . At the bombarding energy used in the present study the $2\alpha2n$ and $2\alpha n$ channels (giving rise to ^{215}Rn and ^{216}Rn), were comparable (the cross sections were estimated to be $\sigma \simeq 20$ and 40 μb respectively). The predominant transitions could be assigned to ^{215}Rn and ^{216}Rn from the coincidence with 2α 's in the E - ΔE matrix of the ISIS array, where the separation between the alpha particles belonging to the $2\alpha2n$ (and $2\alpha n$) channel and the charged particles arising from other reaction channels was very clear. (Only a very small contamination of the $\alpha2n$ channel, leading to ^{219}Ra [10], was present.) Approximately a total of 350 000 events were acquired from the γ - γ - E - ΔE coincidences ($2\alpha xn$ channels, a third of them corresponding to ^{215}Rn). A positive identification of the γ rays from $Z = 86$ nuclei was based on the coincidence between the Rn K x rays and the most intense lines present in the projection spectrum (this is the gamma spectrum in coincidence with 2α hits in the ISIS array, two in the BGO multiplicity filter, and two in the Ge detectors).

In order to determine the multipolarities for the gamma transitions, γ - γ matrices were created by sorting on one axis the detectors lying at $\theta_1 = 31.7^\circ$, 36.0° , 144.0° , and 148.3° and on the other those at $\theta_2 = 90^\circ$ with respect to the beam direction. Due to low statistics of the data only the anisotropy ratios (R), defined as the coincidence intensity ratios of transitions observed in the θ_1 detector rings to those detected in the θ_2 ring with no specific gate, were extracted. In the GASP geometry, the theoretical anisotropy ratios

$I\gamma(\theta_1)/I\gamma(\theta_2)$ are 1 for stretched quadrupole transitions and 0.57 for pure dipole ones. These values are calculated on the basis of the GASP geometry and the directional correlations of gamma radiations emitted from nuclear states oriented by nuclear reactions (see Ref. [11]). This procedure of multipolarity assignment was consistently checked with transitions of known multipolarity belonging to $^{219,220}\text{Ra}$ [10] and the known transitions in ^{216}Rn [12,13].

III. RESULTS

The aim of this section is to establish the new level scheme of ^{215}Rn . A very powerful aid in the construction of the level scheme was the cleanliness of the projection spectrum. Only a few transitions belonging to both ^{215}Rn and ^{216}Rn were contaminated. The isotopic assignment of lines to ^{215}Rn was done on the basis of the reaction energy, the coincidences with Rn K x rays, and the measured coincidence relations with the 316.4 keV ($11/2^+ \rightarrow 9/2^+$) previously observed $M1$ transition [7] in this nucleus. The gamma rays assigned to ^{215}Rn are listed in Table I together with their intensities, anisotropy ratios, and adopted multipolarity. Some

TABLE I. γ -ray energies, intensities, anisotropy ratios R (defined as the intensity ratio of transitions observed in the 31.7° , 36.0° , 144.0° , and 148.3° detector rings to those detected in the 90° ring of the GASP spectrometer) and adopted multiplicities. The data correspond to the $^{207}\text{Pb}(^{18}\text{O},2\alpha2n)$ reaction at 93 MeV bombarding energy.

E_γ^a (keV)	I_γ	R	I^{Tot}	Adopt. mult.
123.2	5(1)		42(9)	($M1$) ^b
158.7	22(6)	1.1(5)		
197.0	9(2)	0.9(0.26)	14(3)	$E2$
203.9	27(6)	0.5(2)	74(16)	$M1$
215.6 ^c	4.3(9)			
230.9 ^c	4.1(9)			
273.6	24(5)	0.92(0.25)	28(6)	$E2$
316.4	25(3)	0.7(2)	37(5)	$M1$ ^d
317.7 ^e	10(2)		15(5)	$M1/E2$
327.4	10(2)		12(2)	($E2$) ^f
376.4	< 2			
383.5	42(8)	0.6(2)	45(9)	
387.2	78(14)	0.9(2)	82(15)	$E2$
388.1 ^e	25(7)		26(8)	($E2$)
446.2	86(6)	0.85(0.15)	88(7)	$E2$
482.3	13(1)		13(1)	($M1/E2$) ^f
570.2	100(5)	1.0(0.15)	100(5)	$E2$
572.5 ^c	5(2)			
629.8	26(3)	0.9(3)	26(3)	$E2$

^aErrors in E_γ are about 0.2 keV.

^bThe electric or magnetic character is deduced from the total intensity balance.

^cTransition belonging to ^{215}Rn which is not included in the present level scheme.

^dMultipolarity known from previous work [6,7].

^eContaminated lines. Relative intensities were deduced from coincidence spectra.

^fMultipolarities in parenthesis are propositions which are not confirmed.

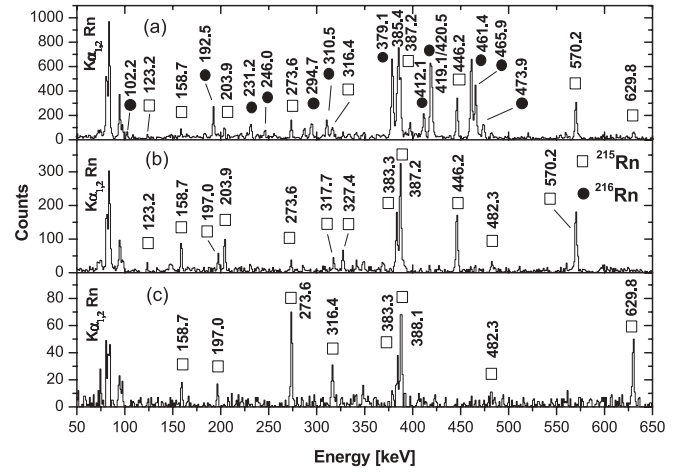


FIG. 1. γ -ray coincidence spectra of Ge detectors corresponding to (a) the γ -ray spectrum gated on the Rn $K_{\alpha,\beta}$ x rays; (b) the sum of coincidence spectra gated on the 570.2 and 446.2 keV transitions assigned to the most intense band A, $9/2^+$, $13/2^+$, $17/2^+$, ..., in the level scheme obtained for ^{215}Rn ; and (c) the sum of coincidence spectra gated on the 316.4 and 629.8 keV transitions assigned to the left-hand side band B, $11/2^+$, $15/2^+$, $19/2^+$, ...

relative gamma-ray intensities were obtained from the total projection of the 2α - γ - γ matrix and others were extracted from coincidence spectra.

Figure 1 shows in panel (a) the γ ray spectrum gated on the Rn $K_{\alpha,\beta}$ x rays; in panel (b) the sum of coincidence spectra gated on the 570.2 and 446.2 keV transitions assigned to the most intense band in the level scheme obtained for ^{215}Rn (see Fig. 2, the structure "A" at the right-hand side); and in panel (c) the sum of coincidence spectra gated on the 316.4 and 629.8 keV transitions assigned to the left-hand side band "B" on the same level scheme. Panels (b) and (c) give part of the

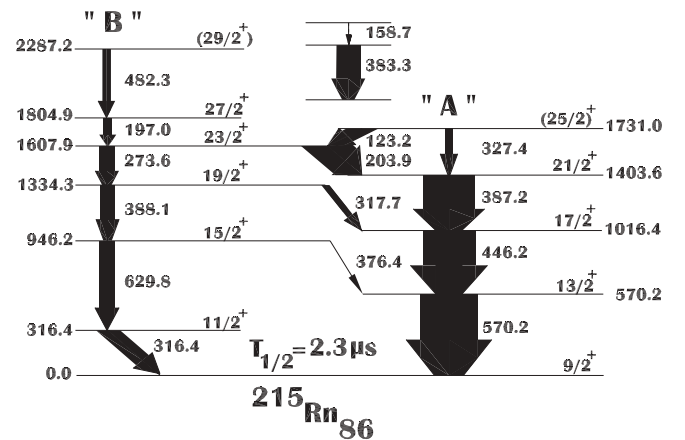


FIG. 2. Level scheme of ^{215}Rn proposed in the present work. Spin assignments are based on $I^\pi = 9/2^+$ ($\nu g_{7/2}^3$ configuration) for the ground state populated by the 570.2 keV first transition of band A and the 316.4 keV transition which connects the band head of band B with the ground state. The relative widths of the arrows indicate the total transition intensities, and correspond to the $^{207}\text{Pb}(^{18}\text{O},2\alpha2n)$ reaction at 93 MeV.

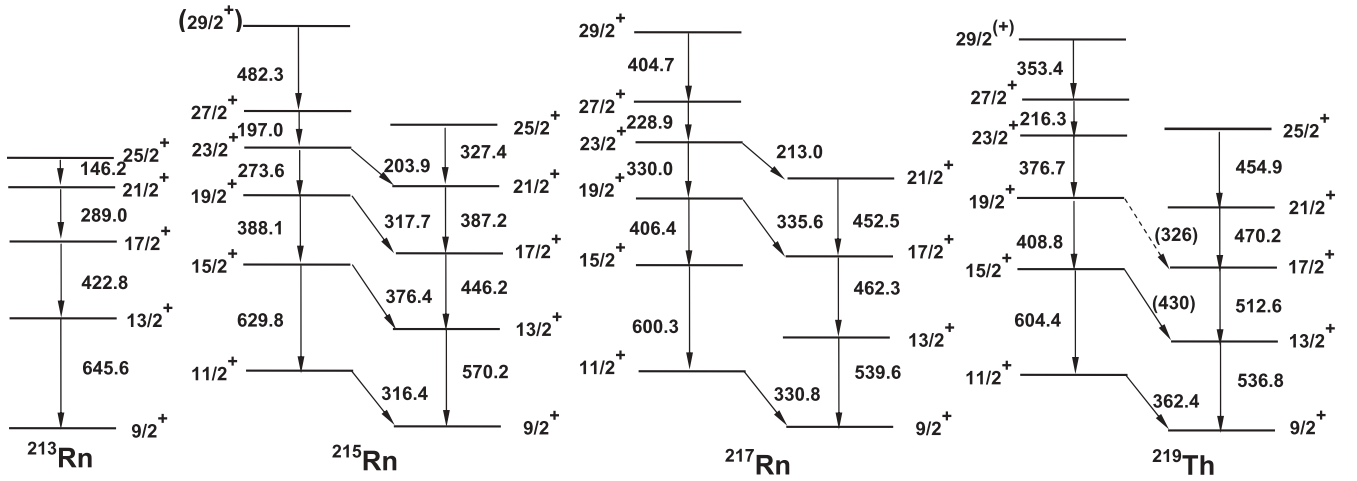


FIG. 3. Comparison of experimental partial level schemes (positive parity states) of the odd $N = 129$ isotones, ^{213}Rn [19], ^{217}Ra [2], ^{219}Th [5], and ^{215}Rn from this work. The figure shows the similarity between the bands in the odd isotones ^{217}Ra , ^{219}Th and the lowest two bands in ^{215}Rn .

relevant experimental evidence on which the construction of the level scheme is based.

Figure 2 shows the experimental level structure of ^{215}Rn obtained from the present study. The ground state is proposed [7] to have spin-parity $9/2^+$, an assignment which is consistent with the $g_{9/2}$ orbit of the spherical shell model for $N = 129$. Also, this same spin-parity was reported in the known $N = 129$ isotones ^{217}Ra [2] and ^{219}Th [5] and in the lighter odd-neutron neighbors. The level scheme consists mainly of two bands connected by the 203.9, 317.7, and 376.4 keV transitions. These bands are strikingly similar to the bands known in its odd isotones ^{217}Ra (Fig. 3) and ^{219}Th . The actual spin and parity assignments (Fig. 2) are based, as far as experimental arguments are concerned, on measured anisotropies and γ - γ intensity balance, and on the justified assumption that this reaction populates the yrast structure of ^{215}Rn . A more detailed discussion follows.

The more intense band starting with the sequence 570.2, 446.2, and 387.2 keV transitions and the sequence starting with the 629.8 keV transition (bands A and B in Fig. 2) were clearly established on the basis of coincidence intensities, anisotropy values, and the existence of the 376.4, 317.7, and 203.9 keV transitions linking both sequences and to the previously known 316.4 keV $M1$ transition [7].

The anisotropy ratio of the 203.9 keV ($23/2^+ \rightarrow 21/2^+$) transition shows a dipole character, within experimental errors, and the intensity balance in the coincidence spectra gated on the 197.0 and 482.3 transitions also supports $M1$ character.

On the other hand, the $M1/E2$ character of the relatively weak 317.7 keV ($19/2^+ \rightarrow 17/2^+$) transition is determined by the coincidence intensity balance. However, it should be mentioned that the $M1/E2$ mixing ratio of the 317.7 keV line has a large uncertainty.

The consistent evidence for a 376.4 keV transition linking the $15/2^+$ state at 946.2 keV and the $13/2^+$ at 570.2 keV level fixes the relative position of the 388.1 and 629.8 keV transitions in the level scheme. The R ratio cannot be reliably

extracted for the 388.1 keV line due to the presence of the much stronger 387.2 keV transition.

In summary, the 570.2, 446.2, and 387.2 keV transitions have stretched $E2$ character, thus fixing the spin-parity sequence of the three first excited states of band A. The 203.9 keV line is a stretched $M1$ dipole which determines the $I^\pi = 23/2^+$ spin-parity of the B band level at 1607.9 keV. For band B, the gamma lines 629.8, 273.6, and 197.0 keV have stretched $E2$ character. Taking into account the coincidence data including the linking 203.9, 317.7, and 376.4 keV transitions and the previously known 316.4 keV line depopulating the $11/2^+$ level at this same energy, the level scheme shown in Fig. 2 follows.

IV. DISCUSSION

The level structure of ^{217}Ra has been interpreted in terms of the shell model by Roy *et al.* [2]. On the other hand, Sheline *et al.* [7] have analyzed the structure of ^{215}Rn and ^{217}Ra from the point of view of the reflection asymmetric model. However, ^{215}Rn is a transitional nucleus between the isotones with $N = 128$, ^{212}Po [14], ^{214}Rn [15], and ^{216}Ra [16], whose properties can be described by two neutrons in the $g_{9/2}$ subshell with the valence protons coupled to zero angular momentum, and the isotones with $N = 130$, ^{216}Rn [13] and ^{218}Ra [17,18], which show collective characteristics. Some of these collective features can also be found in the $N = 129$ isotones.

The 316.4 keV state decays to the ground state through a transition of the same energy, corresponding to the $i_{11/2} \rightarrow g_{9/2}$ neutron transition [7] (similar to the 330.8 keV transition in ^{217}Ra [2,7], the 293.6 keV transition in ^{218}Ac [4], and the 362.4 keV transition in ^{219}Th [5]). This great similarity is fully consistent with the assignments of spins and parities made for ^{215}Rn .

It is interesting to note that the first $\Delta I = 2$ transition energy in ^{215}Rn (570.2 keV) almost coincides with the average of the first transition energies of its neighboring isotopes

$^{214,216}\text{Rn}$, as in the heavier known isotones ^{216}Fr , ^{217}Ra , ^{218}Ac , and ^{219}Th . In addition, the yrast level structure in the $N = 129$ isotones ^{215}Rn , ^{217}Ra , and ^{219}Th shows a significant similarity and a smooth evolution becoming more regular towards larger proton numbers (see Fig. 3).

The ground-state A band ($I^\pi = 9/2^+, 13/2^+, \dots$) starting with the 570.2 keV transition, based mainly on the $\nu g_{9/2}^3$ configuration [7], exhibits more regular spacings than in ^{214}Rn ($N = 128$) and exceeds the maximum spin of $21/2^+$ for that configuration. The $\nu g_{9/2}^3$ configuration is the obvious choice for the largest component of this structure since $g_{9/2}$ is the orbit nearest to the Fermi level. However, $\nu g_{9/2}^3$ alone cannot explain the regular behavior pointing to some quadrupole collectivity onset.

Similarly, the B band ($I^\pi = 11/2^+, 15/2^+, 19/2^+, \dots$) starting with the 629.8 keV transition displays energy spacings decreasing in energy with spin as in ^{214}Rn , seems to terminate at $27/2^+$, and can be most likely interpreted in terms of the $\nu g_{9/2}^2 i_{11/2}$ configuration. Just experimentally, the population path of this nucleus changes from the B band to the A band through the 203.9 keV transition, shifting from the $\nu g_{9/2}^2 i_{11/2}$ to the $\nu g_{9/2}^3$ structure.

The tentative spin and parity ($29/2^+$) assigned to the 2287.2 keV state which is depopulated by the 482.3 keV transition is based on similar transitions 404.7 and 353.4 keV, found in ^{217}Ra [2,7] and ^{219}Th [5] respectively (see Fig. 3).

Whereas in the heavier mass isotones ^{216}Fr , ^{217}Ra , and ^{218}Ac the relative population intensities of the “natural” and “unnatural” parity bands are comparable due to the relative energetic location of these two families of states, no evidence of unnatural parity levels was observed in ^{215}Rn . By “natural” parity states we mean those states having the same parity as the underlying particle configuration. This result is consistent with the measured ^{216}Rn level scheme [13] which shows interleaved bands of alternating parity only above spin 13^- . The striking similarity between ^{216}Fr [1], ^{217}Ra [2], and ^{218}Ac [4], as far as the quadrupole structure is concerned, suggests that the $h_{9/2}$ proton has only a small influence on the evolution of this degree of freedom while it dramatically affects the drop in energy of the unnatural parity states. Additional evidence in this same sense is shown in Fig. 3 in which this evolution is shown for the isotonic chain ^{215}Rn , ^{217}Ra , and ^{219}Th . The addition of the $h_{9/2}$ proton does not modify the “quadrupolar-like structure” already partially developed in ^{215}Rn , but it produces the drastic appearance of the “octupolar structure.” Apparently the appearance of low-lying octupole collectivity requires for $N = 129$ at least five protons ($Z = 87$, ^{216}Fr) and for $Z = 86$ at least five neutrons ($N = 131$, ^{217}Rn [20]) outside the closed shells, as shown in this work and by the results on ^{216}Fr and ^{216}Rn [13].

In order to illuminate the influence of the neutron number, Fig. 4 shows the evolution of the natural and unnatural parity states in the Rn isotopic chain (the states are labeled by the spin and parity differences with respect to the I_g “band head” state; $I_g = 9/2^+$ for ^{215}Rn), showing a typical behavior of monotonic decrease and compression of the transitions and level energies reflecting a quite sensitive behavior of the quadrupole degree of freedom as one moves away in neutron number from the closed shell $N = 126$, in contrast to the proton-number dependence.

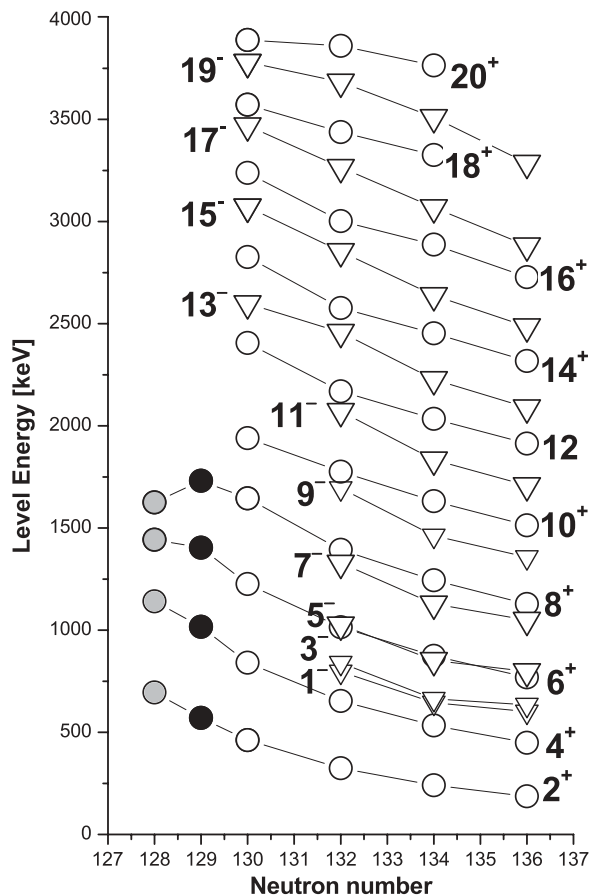


FIG. 4. Yrast level systematics for excited states of Rn isotopes as function of neutron number. Inverted triangles correspond to odd spin states, and circles to even spin states. Empty symbols are data from Ref. [21] ($^{218,220,222}\text{Rn}$) and Ref. [13] (^{216}Rn), full gray symbols are taken from Ref. [15] (^{214}Rn), and full black symbols are data obtained in this work. The states are labeled by $(I - I_g)^\pi$ where I represents the spins of the excited levels of the ground-state bands, I_g the spins of the band head states, and $\pi = +1$ (-1) for even (odd) parity states respectively.

It follows from this systematics that for the Rn isotopes the quadrupole collectivity appears at $N = 129$ whereas the octupole collectivity starts at low spins just at $N = 131$.

V. SUMMARY AND CONCLUSIONS

High spin states in ^{215}Rn were populated through the $^{207}\text{Pb}(^{18}\text{O}, 2\alpha 2n)$ reaction and studied using the 8π GASP-ISIS spectrometer at Legnaro. In order to achieve a clean spectroscopy and resolve the transitions of interest from the intense gamma background originated from fission, we trigger the gamma detectors of the GASP spectrometer with the $E-\Delta E$ particle detectors of the ISIS array, selecting the evaporation of particles emitted in coincidence with transitions between excited states in ^{215}Rn . The close correspondence between the experimentally determined ^{217}Ra and ^{215}Rn level schemes, the previously performed work in this region [2,7], and the restricted set of available single-particle states around the

Fermi surface strongly suggest for ^{215}Rn the same positive parity yrast structure as the one previously assigned to ^{217}Ra . In line with the experimental ^{216}Rn level scheme [13], no negative-parity low-lying levels have been found here in ^{215}Rn .

The results of this and previous studies [1] probably indicate lower limits $Z \geq 87$ and $N = 129$ for the region in which the development of the quadrupolar and octupolar collectivity starts.

-
- [1] M. E. Debray, J. Davidson, M. Davidson, A. J. Kreiner, D. Hojman, D. Santos, K. Ahn, D. B. Fossan, Y. Liang, R. Ma, E. S. Paul, W. F. Piel, and N. Xu, *Phys. Rev. C* **41**, R1895 (1990).
- [2] N. Roy, D. J. Decman, H. Kluge, K. H. Maier, A. Maj, C. Mittag, J. Fernández Niello, H. Puchta, and F. Riess, *Nucl. Phys. A* **426**, 379 (1984).
- [3] M. E. Debray, M. Davidson, A. J. Kreiner, J. Davidson, G. Falcone, D. Hojman, and D. Santos, *Phys. Rev. C* **39**, R1193 (1989).
- [4] M. Debray, A. J. Kreiner, M. Davidson, J. Davidson, D. Hojman, D. Santos, V. R. Vanin, N. Schulz, A. Chevallier, and J. Chevallier, *Nucl. Phys. A* **568**, 141 (1994).
- [5] W. Reviol, D. G. Sarantites, C. J. Chiara, M. Montero, R. V. F. Janssens, M. P. Carpenter, T. L. Khoo, T. Lauritsen, C. J. Lister, D. Seweryniak, S. Zhu, O. L. Pechenaya, and S. G. Frauendorf, *Phys. Rev. C* **80**, 011304(R) (2009).
- [6] A. M. Y. El-Lawindy, J. D. Burrows, P. A. Butler, J. R. Cresswell, V. Holliday, G. D. Jones, R. Tanner, R. Wadsworth, D. L. Watson, K. A. Konell, J. Simpson, C. Lauterbach, and J. R. Mines, *J. Phys. G* **13**, 93 (1987).
- [7] R. K. Sheline, C. F. Liang, P. Paris, A. Gizon, and V. Barci, *Phys. Rev. C* **49**, 725 (1994).
- [8] E. Browne, *Nucl. Data Sheets* **65**, 669 (1992).
- [9] D. Hojman *et al.*, *Phys. Rev. C* **73**, 044604 (2006).
- [10] P. D. Cottle, M. Gai, J. F. Ennis, J. F. Shriner Jr., D. A. Bromley, C. W. Beausang, L. Hildingsson, W. F. Piel Jr., D. B. Fossan, J. W. Olness, and E. K. Warburton, *Phys. Rev. C* **33**, 1855 (1986).
- [11] K. S. Krane, R. M. Steffen, and R. M. Wheeler, *Nucl. Data* **11**, 351 (1973).
- [12] P. D. Cottle, M. Gai, J. F. Ennis, J. F. Shriner Jr., S. M. Sterbenz, D. A. Bromley, C. W. Beausang, L. Hildingsson, W. F. Piel Jr., D. B. Fossan, J. W. Olness, and E. K. Warburton, *Phys. Rev. C* **35**, 1939 (1987).
- [13] M. E. Debray, J. Davidson, M. Davidson, A. J. Kreiner, M. A. Cardona, D. Hojman, D. R. Napoli, S. Lenzi, G. de Angelis, D. Bazzacco, S. Lunardi, M. De Poli, C. Rossi-Alvarez, A. Gadea, N. Medina, and C. A. Ur, *Phys. Rev. C* **73**, 024314 (2006).
- [14] A. R. Poletti, G. D. Dracoulis, A. P. Byrne, and A. R. Stuchbery, *Nucl. Phys. A* **477**, 595 (1987).
- [15] G. D. Dracoulis, A. P. Byrne, A. R. Stuchbery, R. A. Bark, and A. R. Poletti, *Nucl. Phys. A* **467**, 305 (1987).
- [16] T. Lonnroth, D. Horn, C. Baktash, C. J. Lister, and G. R. Young, *Phys. Rev. C* **27**, 180 (1983).
- [17] J. Fernández Niello, H. Puchta, F. Riess, and W. Trautmann, *Nucl. Phys. A* **391**, 221 (1982).
- [18] M. Gai, J. F. Ennis, M. Ruscev, E. C. Schloemer, B. Shivakumar, S. M. Sterbenz, N. Tsoupras, and D. A. Bromley, *Phys. Rev. Lett.* **51**, 646 (1983).
- [19] T. Lönroth and C. Baktash, *Physica Scripta*. **28**, 459 (1983).
- [20] M. E. Debray *et al.* (unpublished).
- [21] J. F. C. Cocks, D. Hawcroft, N. Amzal, P. A. Butler, K. J. Chan, P. T. Greenlees, G. D. Jones, S. Asztalos, R. M. Clark, M. A. Deleplanke, R. M. Diamond, P. Fallon, I. Y. Lee, A. O. Macchiavelli, R. W. MacLeod, F. S. Stephens, P. Jones, R. Julin, R. Broda, B. Fornal, J. F. Smith, T. Lauritsen, P. Bhattacharyya, and C. T. Zhang, *Nucl. Phys. A* **645**, 61 (1999).